

Vibration sensor with tunable signals using bundled fiber probe

M. YASIN^{a,*}, M. ZULKARNAEN^a, SAMIAN^a, A. H. ZAIDAN^a, Y. G. Y. YHUWANA^a, H. TRILAKSANA^a, S. W. HARUN^{a,b}

^a*Department of Physics, Faculty of Science and Technology, Airlangga University, Surabaya 60115, Indonesia*

^b*Department of Electrical Engineering, University of Malaya, 50603 Kuala Lumpur, Malaysia*

A low cost and simple vibration sensor with tunable signals is proposed and demonstrated based on the principle of extrinsic reflective intensity modulation of displacement measurement for monitoring the heart beat. The front slope of the displacement sensor has a sensitivity of 0.44 mV/ μm and linearity of 88% within a measurement range between 0 and 100 μm , while for the back slope, it shows a sensitivity of 0.06 mV/ μm and linearity of 97% within a range from 150 μm to 750 μm . By placing the diaphragm of the concave surface loudspeaker within the linear range (in the back slope) from the probe, the vibration frequency of the object can be measured with an error percentage of less than 0.2%. The graphs of three various inputs against outputs frequency in sine, square, and triangle waveform show very high linearity up to 99%. Slope for tunable signals (e.g. sine, square and triangle frequency range) is obtained at 0.98 for all waveforms. Effortlessness, long-haul security, low power utilization, wide frequency ranges, lower noise, toughness, linearity and light weight make it a promising candidate in contrast to other well-set up strategies for vibration frequency detection.

(Received February 1, 2019; accepted October 9, 2019)

Keywords: Fiber optic, Fiber optic vibration sensor, Bundled probe and tunable signals

1. Introduction

Fiber-optic have been widely used in various areas such as communication, information transmission and sensor. Recently, many works have been reported on fiber-optic sensors for measuring displacement, weight, temperature, electric field, etc [1-3]. Compared to the conventional electrical based sensors, fiber-optic sensors are preferable due to their advantages of excellent electrical isolation, immunity from electromagnetic fields, compactness, and compatibility with other optical fiber devices.

One of the important applications of the fiber-optic sensors is in the area of vibration analysis. Vibration detection is required in numerous applications including medical cases (e.g. heart rate signal), automotive industry, aircraft, and other high precision technology. In recent years, various fiber-optic vibration sensors have been proposed and fabricated based on different approaches such as fiber interferometry technique [4], fiber Bragg grating (FBG) [5], over-coupled fused coupler (OCFC) [6] and also bundled optical fiber [7]. The fiber interferometers operate based on the phase modulation of the input signal and thus it is complicated to implement on-site, rather expensive and prone to temperature fluctuation [8]. FBG sensor must use mechanical devices to improve their sensitivity, while the use of OCFC requires three fiber lines to transmit the input and output of the sensor. Bundled fiber based sensors can operate within low frequency range (less than 500 Hz) [7, 9].

On the other hand, plastic optical fibers (POFs) have gain a tremendous interest in recent years due to their great

demands for the transmission and processing of optical signals in the optical fiber communication system [10]. Furthermore, they are inexpensive and have high mechanical flexibility and numerical aperture. An intensity modulated fiber optic displacement sensor has also been demonstrated to be efficient for different applications. They are relatively inexpensive, easy to fabricate, and suitable for employment in harsh environments. Up to date, many non-contact vibration sensors were demonstrated using bifurcated bundle POF based on the principle of extrinsic reflective intensity modulation [11-13]. These sensors are advantageous for various applications due to its simplicity, low-cost, immunity to electromagnetic interference, and the possibility of distributed and long term vibration monitoring over a single optical fiber link.

In our previous work, a vibration sensor was also demonstrated based on displacement measurement [14]. The sensor is capable of measuring vibration amplitude ranging from 0.22 mm to 0.44 mm within a frequency range of 200 to 350 Hz. In this paper, a relatively simple, low cost, yet very efficient vibration sensor is proposed and demonstrated based on similar technique for application in heart beat detection. Compared to the previous work [14], this sensor can measure a low frequency range, which is suitable for application in heart beat detection. The proposed sensor was successfully used to measure vibration frequency of a loudspeaker ranging from 50 to 100 Hz.

2. Experimental setup

Fig. 1 shows the experimental set-up for the proposed fiber displacement vibration sensor. It consists of a 633nm light source, bundled plastic optical fiber, loudspeaker, audio generator, silicon-photo detector, and a digital storage oscilloscope. Two meters long bundled fiber consisting one transmitting fiber (TF) with 1.0mm and 16 receiving fibers (RF) with 0.25mm in diameter respectively, was used as a probe. The light source used in this study is a He-Ne laser with a peak wavelength of 633 nm. Silicon photo-detector was employed as it provides high speed detection with an optical response from 400nm to 1100 nm, enabling to be compatible with a wide range of visible light wavelength including the 633 nm visible He-Ne laser employed in this experiment.

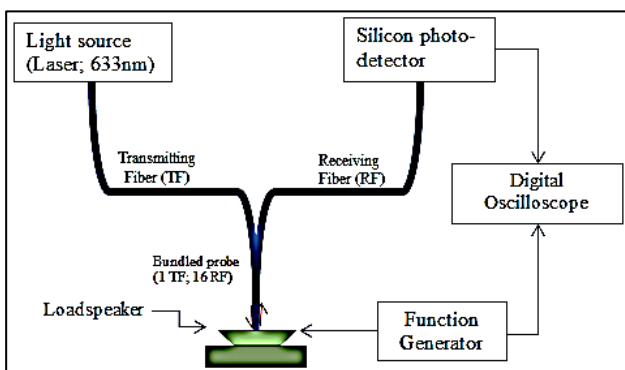


Fig. 1. Experimental setup

The light from He-Ne laser enters the transmitting fiber line and then radiates to the concave diaphragm of the loudspeaker, and the reflected beam from the diaphragm is transmitted through the receiving fiber line to the silicon photo-detector. Firstly, the calibration measurement was performed for the diaphragm of the loudspeaker at zero vibration frequency. The amplitude of the output signal is measured from the digital storage oscilloscope for every $50\mu\text{m}$ increase in displacement from the diaphragm of the loudspeaker. A graph of intensity output signal against displacement is drawn and the linear range on the front slope region is identified. Then an experiment is carried out where the speaker is turned on to emit signals of different frequencies controlled by the tunable function generator. The input signal with sinusoidal shape was used throughout the experiment. The selected frequency range as data sampling is ranging from 50 to 100 Hz for sine, square, and triangle waveforms. For each input frequency, the frequency of output signal was measured from the digital oscilloscope. The working principle of the sensor was theoretically described in ref. [15].

3. Results and discussions

Fig. 2 shows the variation of the output voltage signal against displacement from the diaphragm of the loudspeaker at zero vibration frequency (i.e. when the speaker is off). The output signal is minimum at zero displacement because the light cone does not reach the RF cores. By increasing the displacement, the volume of the reflected beam cone increases and starts overlapping with RF cores thus gives a small output signal. Larger overlapping volume leads to further increase in the output signal until it reaches the maximum value where the reflected cone power falls within the surface area of the RF. Beyond the peak value of displacement, the reflected cone size is bigger than the size of the RF. Therefore, only a fraction of the power of the reflected light will be detected, where its effect can be seen as almost an inverse square law relationship between the output signal and the displacement. A linear range of linearity more than 88 % is obtained in the front slope of the profile as shown in Fig. 2. A very short linear range was obtained. Therefore, this range can not be used as the position of the probe for vibration measurement. For the back slope, a linear range of $600\mu\text{m}$ was obtained starting from the distance of $150\mu\text{m}$ to $750\mu\text{m}$ with the sensitivity of the back slope is calculated as $0.06\text{ mV}/\mu\text{m}$.

Table 1 summarizes the performance of the displacement sensor in the front and back slope regions. The back slope linear region with lower sensitivity will be used in the vibration sensor measurement. In this work, the initial position of the loudspeaker is fixed within the linear range of the back slope for vibration measurement. The stability measurement of the sensor's output signal at the initial position is shown in the insert of Fig. 2. We obtain a very stable output voltage for the displacement sensor system with the measurement error of less than 0.2% when the loudspeaker is turned off.

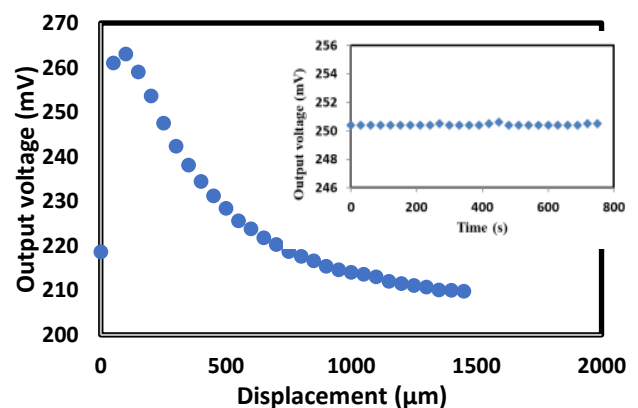


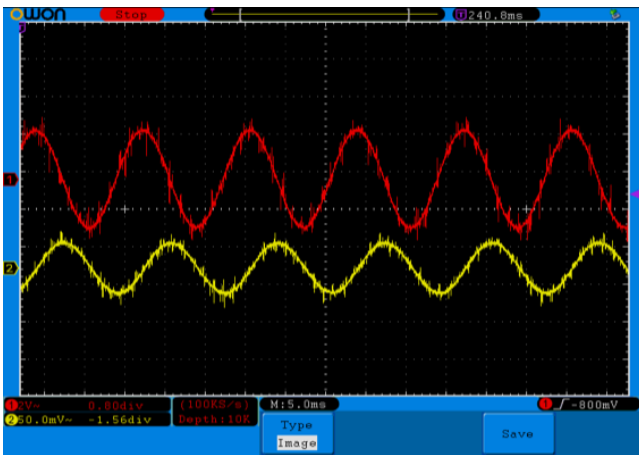
Fig. 2. The variation of the output voltage with the displacement of the fiber optic probe from the diaphragm of the load-speaker. Inset shows the stability of the sensor with error measurement of 0.05mV

Table 1. The linear region of fiber optic displacement sensor

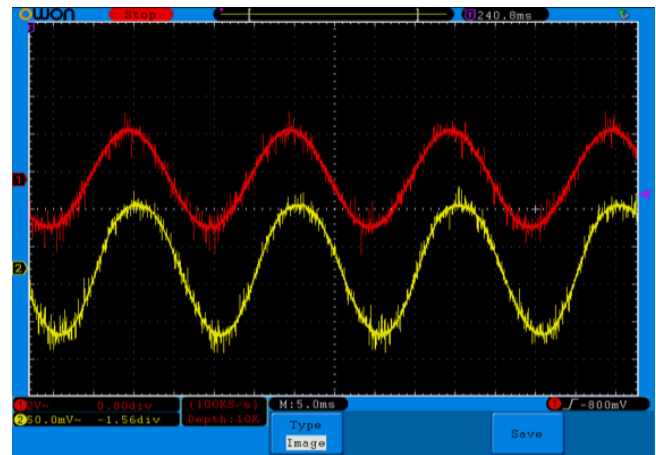
Front slope			Back slope		
Sensitivity (mV/ μ m)	Linear range (μ m)	Resolution (μ m)	Sensitivity (mV/ μ m)	Linear range (μ m)	Resolution (μ m)
0.444	0-100	0.1	0.066	150-750	0.76

Figs. 3, 4, and 5 show the measured frequency of the loudspeaker against the input driving frequency of the audio generator for sine, square and triangle signals, respectively. In this experiment, the gap between the mirror and fiber bundle probe is fixed at the back slope range (150-750 μ m), which is the linear range of displacement sensor when the speaker is off. The speaker frequency is varied from 50 to 100 Hz, 50 to 80 Hz and 50 to 80 Hz for sine, square and triangle signals respectively.

As can be seen from Figs. 3, 4 and 5, the output signal carries the same sinusoid, square and triangle shape as the input signal for each measurement. Figs. 6(a), 7(a) and 8(a) show the relation between the input and output frequency of the sensors with sine, rectangular and triangle signal respectively. As shown in these figures, the input frequency seems to be similar compared to the output frequency with a linearity of more than 98% for all frequency shapes. Figs. 6(b), 7(b) and 8(c) show the relation between the input and output amplitude of the sensors with sine, rectangular and triangle signal respectively. As shown in these figures, the measured output amplitudes are showing that it has a linear function trend as a function of the input amplitude with slope obtained is more than 90% for all frequency shapes. The performance of fiber optic vibration frequency sensor is then summarized in Table 2. The stability measurement of the sensor's is also investigated, which indicates the percentage of the measurement error of less than 0.2%.

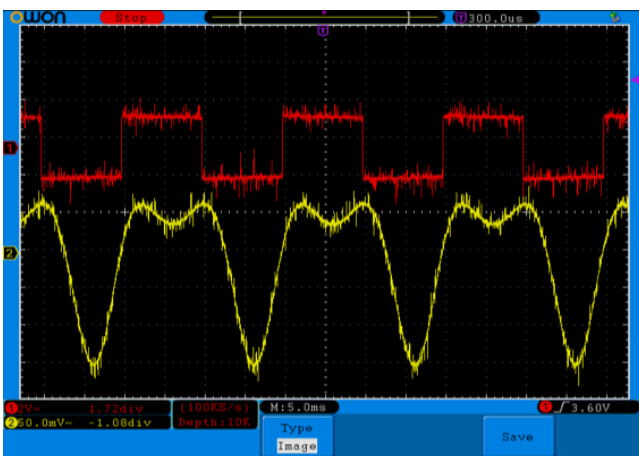


(a)

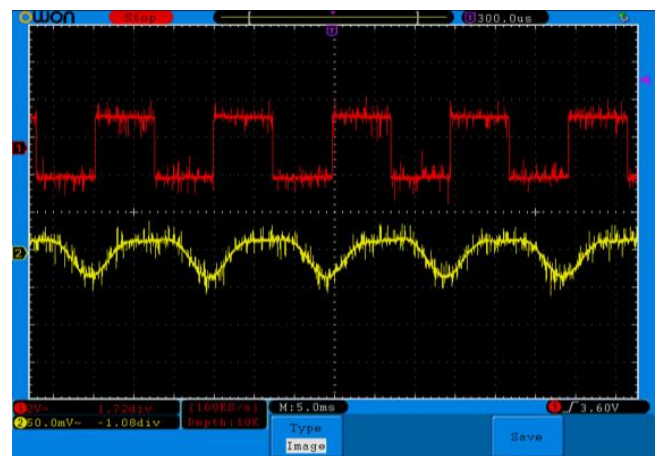


(b)

Fig. 3. The digital oscilloscope display of the input and output sine signal representation for (a) 50 Hz and (b) 75 Hz

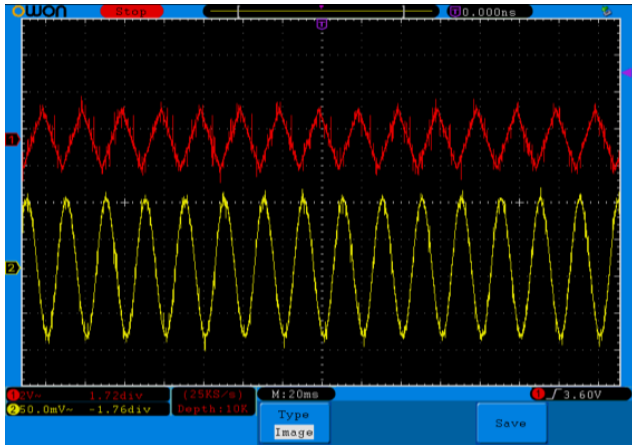


(a)

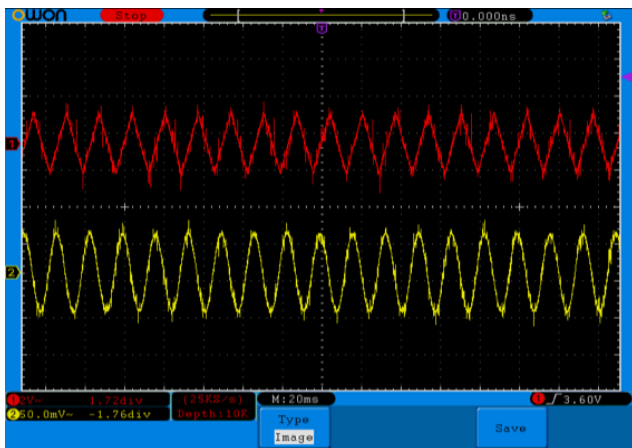


(b)

Fig. 4. The digital oscilloscope display of the input and output square signal representation for (a) 50 Hz and (b) 68 Hz



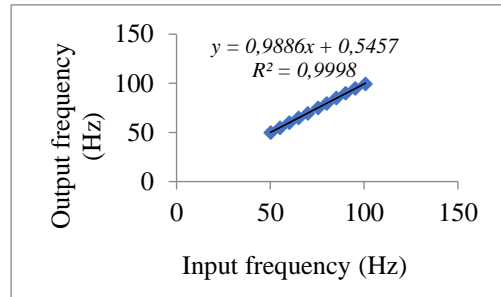
(a)



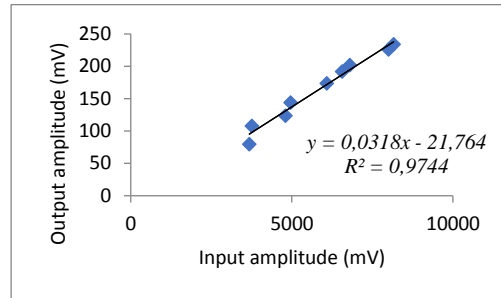
(b)

Fig. 5. The digital oscilloscope display of the input and output triangle signal representation for (a) 50 Hz and (b) 60 Hz

The results indicates that the developed sensor system is capable to measure a high performance frequency vibration as well as to be able to detect the sinusoid, square, and triangle shape of the input vibration signals. The sensor configuration is designed so that the ambient condition is constant throughout the experiment thus minimizing its effect on the output signal. To reduce the mechanical vibration, the set up of the experiment has been primarily rigidly attached to the vibration free table. The sensor system is very suitable for real field applications due to its simplicity, high sensitivity as well as low cost of the fabrication.

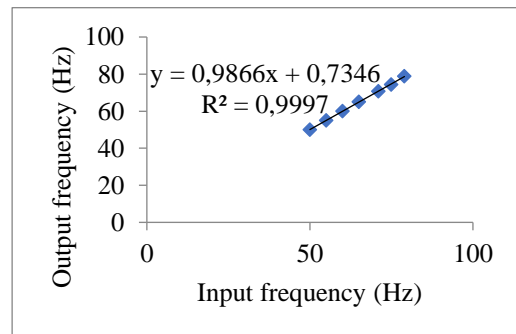


(a)

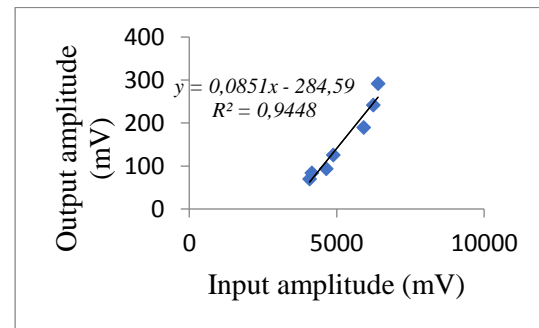


(b)

Fig. 6. The graph of (a) frequency of the output signal against the frequency of given input sine from 50 to 100 Hz and (b) amplitude of output signal against the amplitude of given input sine at 50 Hz

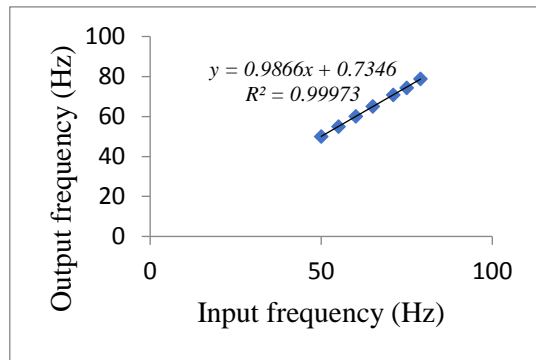


(a)

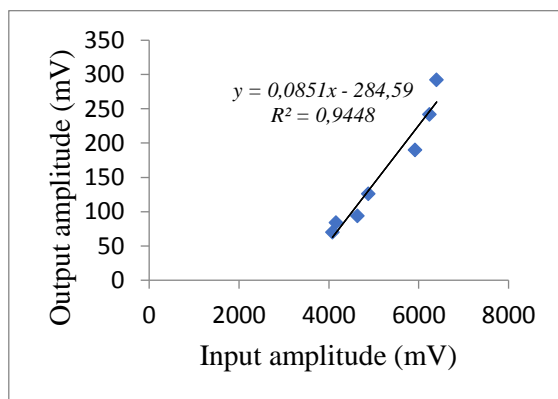


(b)

Fig. 7. The graph of (a) frequency of output signal against the frequency of given input square from 50 to 80 Hz and (b) amplitude of output signal against the amplitude of given input square at 50 Hz



(a)



(b)

Fig. 8. The graph of (a) frequency of the output signal against the frequency of giving an input triangle from 50 to 80 Hz and (b) amplitude of output signal against the amplitude of given an input triangle at 50 Hz

Table 2. Performance of the tunable vibration frequency sensor

Tunable frequency shape	Sine waveform (50-100 Hz)	Square waveform (50-80 Hz)	Triangle waveform (50-80 Hz)
Linearity	More than 99 %	More than 99 %	More than 99 %
Slope	0.98	0.98	0.98

4. Conclusions

An extrinsic fiber optic vibration sensor is proposed and investigated to measure a tunable vibration frequency ranging from 50 to 100 Hz based on fiber optic displacement sensor using a polymer multimode bundled fiber as a probe. The front slope displacement sensor has a sensitivity of 0.44 mV/ μm and linearity of 88 % within a measurement range between 0 and 100 μm . By placing the diaphragm of the concave load-speaker within the linear range of the probe, the frequency of the tunable vibration can be determined. The graph of the input against the output frequency of sine, square, and triangle waveform frequency, shows very high linearity of more than 0.98. Simplicity, long term stability, low power consumption, wide dynamic and frequency ranges, noise reduction,

ruggedness, linearity and light weight enabling it as a promising alternative to other well-established methods for vibration frequency measurement.

Acknowledgements

This work was supported by Indonesia Government through Competencies Based Research Grant (PBK; No. 01/E/KPT/ 2018) and Airlangga University Grant (2018).

References

- [1] S. Maske, P. B. Buchade, A. D. Shaligram, Optics and Laser Technology **98**, 339 (2018).
- [2] Q. Zhao et al., Sensors and Actuators A: Physical **280**, 68 (2018).
- [3] F. Xu et al., Microwave and Optical Technology Letters **56**(12), 2778 (2014).
- [4] P. Wei, X. Shan, X. Sun, Optical Fiber Technology, **19**, 1 (2013).
- [5] Y. Guozhen, L. Yongqian, Y. Zhi, Optik **127**(20), 8874 (2016).
- [6] R. Chen et al., Measurement Science and Technology **15**(8), 1490 (2004).
- [7] H. Zhang, R. Kuschmierz, J. Czarske, Optics and Lasers in Engineering **107**, 364 (2018).
- [8] Y. Zhao et al., Sensors and Actuators A: Physical **273**, 107 (2018).
- [9] Y. G. Y. Yhuwana, R. Apsari, M. Yasin, Optik **134**, 28 (2017).
- [10] H. Z. Yang, S. W. Harun, H. Ahmad, Sensor Review, **31**(1), 65 (2011).
- [11] Miodrag G. Jelić, Dragan Z. Stupar, Bojan M. Dakić, Jovan S. Bajić, Miloš P. Slankamenac, Miloš B. Živanov, 2012 IEEE 10th Jubilee International Symposium on Intelligent Systems and Informatics, September 20-22, 2012, Subotica, Serbia.
- [12] P. Kishore, D. Dinakar, M. Sai Shankar, K. Srimannarayana, P. Vengal Rao, D. Sengupta, International Journal of Optoelectronic Engineering **2**(1), 4 (2012).
- [13] P. Kishore, D. Dinakar, M. Sai Shankar, K. Srimannarayana, P. Vengal Rao, D. Sengupta, P. Saidi Reddy, Proc. of SPIE-OSA-IEEE Asia Communications and Photonics **8311**, 83110P.
- [14] M. Yasin, S. W. Harun, Kusminarto, H. Ahmad, Optoelectron. Adv. Mat. **4**(11), 1795 (2010).
- [15] M. Yasin, S. W. Harun, Kusminarto, Karyono, A. H. Zaidan, K. Thambiratnam, H. Ahmad, Fiber and Integrated Optics **28**, 301 (2009).

*Corresponding author: yasin@fst.unair.ac.id